Available online at www.sciencedirect.com

SciVerse ScienceDirect

Ceramics International 39 (2013) 4695–4700

CERAMICS INTERNATIONAL

www.elsevier.com/locate/ceramint

Short communication

Synthesis of highly sinterable Yb:Sc_2O_3 nanopowders for transparent ceramic

Xiao Lu[a,b], Benxue Jiang[a,*], Jiang Li[a], Wenbin Liu[a], Liang Wang[a], Xuewei Ba[a], Chen Hu[a], Binglong Liu[a], Yubai Pan[a]

[a]*Key Laboratory of Transparent and Opto-functional Inorganic Materials, Shanghai Institute of Ceramics, Chinese Academy of Sciences, 1295 Ding Xi Road, Shanghai 200050, PR China*

[b]*Graduate School of the Chinese Academy of Sciences, 19A Yuquan Road, Beijing 100039, PR China*

Received 10 October 2012; received in revised form 30 October 2012; accepted 31 October 2012
Available online 12 November 2012

Abstract

Ytterbium doped scandium oxide (Yb:Sc_2O_3) nanopowders were synthesized by a novel co-precipitation method. A NH_4HCO_3+NH_4OH (molar ratio=3:1) mixed solution was adopted as the precipitant. The characteristics of precursor and powders calcined at different temperatures were investigated. After calcination at 1100 °C for 4 h, highly sinterable Yb:Sc_2O_3 nanopowders with primary particle size of about 35 nm and low agglomeration were obtained. Using as prepared powders, high optical quality Yb:Sc_2O_3 transparent ceramic with average grain size of about 10 μm was fabricated by vacuum sintering at 1700 °C for 20 h. The in-line transmittance of the sample (1.0 mm in thickness) reached 71.6% at the wavelength of 1200 nm. The spectroscopic properties of the transparent ceramic were also studied.

Keywords: Yb:Sc_2O_3; Transparent ceramics; Co-precipitation method; Mixed precipitant

1. Introduction

To achieve a high-power short-pulse laser, a broad emission spectrum and favorable thermal properties are important [1]. Trivalent ytterbium (Yb^{3+}) is believed to be one of the most attractive materials to satisfy those needs. Because Yb^{3+} has only two manifolds, the ground state $^2F_{7/2}$ and upper level $^2F_{5/2}$, there is no intrinsic process for concentration quenching. Yb^{3+} also owns high quantum efficiency, large crystal-field splitting and broad absorption and fluorescence spectra [2,3]. Among Yb^{3+} doped materials, Yb:Sc_2O_3 probably holds the greatest promise because of its large emission cross section, large splitting of the ground state and high thermal conductivity at low Yb-doping levels [4].

Due to its high melting point (~2430 °C), the study on Sc_2O_3 is mainly focused on transparent ceramics [5]. As we know, high purity, good dispersibility and uniform size are benefit to the powders sinterability, which is a promise for the fabrication of high optical quality transparent ceramics. Recently, a lot of methods have been tried to synthesize Sc_2O_3 nanopowders, such as pyrolysis [6], sol–gel process [7], precipitation [8–12], Pechini method [13]. Among these methods, precipitation has been verified to be an ideal method for preparation of Sc_2O_3 nanopowders with favorable properties due to its convenience and low cost. But the synthesis process and the sinterability of powders still need to be improved.

In this work, 5 at% Yb:Sc_2O_3 nanopowders were synthesized via a novel co-precipitation method and the corresponding transparent ceramics were fabricated by vacuum sintering. A mixed solution of analytical grade ammonium hydrogen carbonate (NH_4HCO_3) and ammonium hydroxide (NH_4OH) was adopted as the precipitant. The effects of the calcination temperature on phase, particle size, and morphology of the Yb:Sc_2O_3 powders were investigated. The microstructures and optical properties of the sintered Yb:Sc_2O_3 ceramics fabricated at different temperatures were also studied.

*Corresponding author. Tel.: +86 21 52412816; fax: +86 21 52413903.
E-mail address: jiangsic@foxmail.com (B. Jiang).

0272-8842/$ - see front matter © 2012 Elsevier Ltd and Techna Group S.r.l. All rights reserved.
http://dx.doi.org/10.1016/j.ceramint.2012.10.268

2. Experimental

2.1. Powders synthesis and transparent ceramics fabrication

The raw materials were commercial Sc_2O_3 and Yb_2O_3 powders (Sigma-Aldrich Chemicals, USA, 99.99% pure). $Sc(NO_3)_3$ and $Yb(NO_3)_3$, as the starting salts, were made by dissolving the oxide powders in an excess amount of nitric acid (Shanghai Lingfeng Chemical Reagent Co., Ltd., analytical reagent) according to the formula $(Yb_{0.05}Sc_{0.95})_2O_3$ at about 80 °C. The excess acid was finally removed by evaporating the salt solution to dryness. Then the nitrate salts were dissolved into distilled water as mother solution with 5 wt% ammonia sulfate ($(NH_4)_2SO_4$) added as the dispersant. The Yb:Sc_2O_3 precursor was prepared at 5–8 °C by dripping a 1 M mixed analytical grade NH_4HCO_3 and NH_4OH solution (molar ratio = 3:1) into a 0.3 M Sc^{3+} mother solution at a rate of 3 ml/min under mild stirring until the pH value of the solution reached 7. After aging at the reaction temperature for 3 h, the suspension was filtered using centrifugal filtration, washed four times with deionized water, twice with anhydrous ethanol to remove the byproducts and then dried at 70 °C in air. After being crushed and sieved through 200 meshes, the precursor was calcined at different temperatures for 4 h to form Yb:Sc_2O_3 powders. The obtained powders were dry-pressed in a stainless-steel die with a diameter of 18 mm followed by cold isostatic pressing (CIP) at 250 MPa to form green compacts. The compacts were sintered at different temperatures for 20 h under $\sim 5 \times 10^{-3}$ Pa vacuum. Finally, the vacuum sintered samples were annealed at 1450 °C for 10 h in air then mirror-polished and thermal etched for characterizations.

2.2. Characterization

Fourier transform infrared spectroscopy (FTIR) analysis was performed on an infrared spectrometer (VERTEX-70) spectrometer. Differential thermal analysis and thermogravimetry (DTA/TG) curves were recorded on a NETZSCH STA 449C instrument at a heating rate of 10 °C/min. X-ray diffractometry (XRD) analysis was carried out on a diffractometer in the range of $2\theta = 10–80°$ using nickel-filtered Cu K_α radiation at the scanning speed of 8°/min (2θ). The specific surface area (S_{BET}) of the Yb:Sc_2O_3 powders was measured by the Brunauer–Emmett–Teller (BET, *V*-Sorb 2800P, Gold APP, China). The morphologies of the Yb:Sc_2O_3 powders and thermal etched surfaces of obtained ceramics were characterized using a field emission scanning electron microscope (FESEM, Magellan 400). The in-line transmittance at room temperature and absorption spectrum of mirror-polished specimen (1.0 mm in thickness) were measured by UV–VIS–NIR spectrophotometer (Model Cray-5000, Varian, CA, USA). The emission spectrum was recorded by a spectrofluorometer (Model SPEX Fluorolog-3, Jobin Yvon, France) employing a photomultiplier (Model R5509-72, Hammatsu, Japan) as the light detector and with 896 nm InGaAs LD as the pump source.

3. Results and discussion

Fig. 1 shows DTA/TG curves of the precursor. DTA curve shows an endothermic peak at about 120 °C corresponding to the release of absorbed water. The exothermic peak at about 670 °C is due to the crystallization process of Yb:Sc_2O_3. TG curve indicates the precursor decomposes to oxides via three major steps. The first step below 650 °C is mainly due to evaporation of release of hydration water and OH^-. The second step at the temperature range of 650–850 °C is largely for decomposition of the carbonate. The mass loss above 850 °C is mainly owing to sulfurization which is the third step. It is found that thermal decomposition of the precursor into Yb:Sc_2O_3 powders is almost completed at ~1100 °C since there is no significant weight loss higher than that temperature.

Fig. 2 shows FTIR spectra of the precursor and its calcination products. The absorption band at ~1640 cm^{-1} is characteristic of H–O–H bending mode of molecular

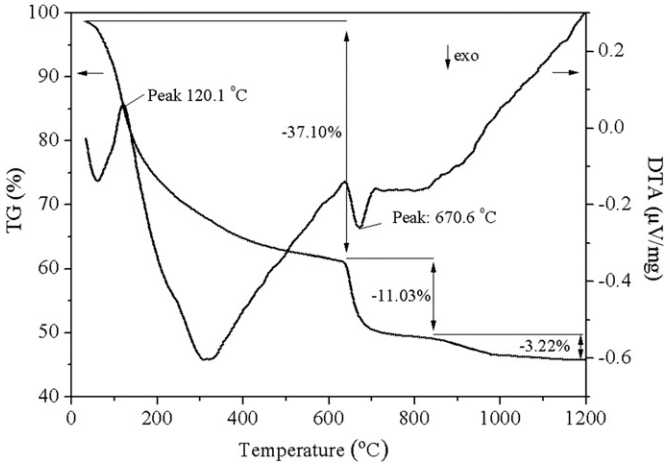

Fig. 1. DTA/TG curves of the Yb:Sc_2O_3 precursor.

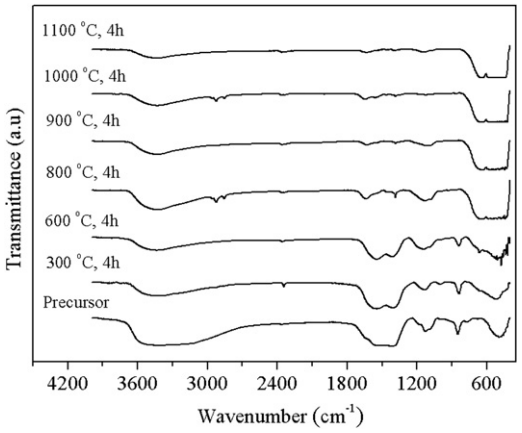

Fig. 2. FTIR spectra showing the decomposition process of the as-synthesized precursor.

water. The broad-band peaking at $\sim$3430 cm^{-1} is associated with the coupled effects of molecular water and free hydroxyl groups (hydroxyls coordinated with scandium ions but not part of molecular water) [8]. The two intense peaks at 1550 and 1402 cm^{-1} are assigned to the asymmetric stretch of the C–O bond in CO_3^{2-}, while the peaks at 837 cm^{-1} are due to the deformation vibration of C–O in CO_3^{2-} [14]. The peaks at around $\sim$1100 cm^{-1} are associated with SO_4^{2-} [15]. As the temperature increases, intensities of the peaks of H_2O, OH^- and CO_3^{2-} decrease clearly, which indicates a gradual dehydration, dehydroxylation and decarburization exists below 800 °C. As the intensities of SO_4^{2-} bands obviously reduce above 900 °C, it shows desulphurization starting at 800–900 °C. Furthermore, the new absorption band near 637 cm^{-1} is attributed to the characteristic stretching of the Sc–O bond, resulting from the crystallization of Yb:Sc_2O_3 from the precursor [16]. Only Sc–O vibration band is found in the powder calcined at 1100 °C, implying the high purity of the Yb:Sc_2O_3 powders at this temperature. The above FTIR result is consistent well with the DTA/TG result.

X-ray diffraction (XRD) patterns of the precursor and the powders calcined at various temperatures are shown in Fig. 3. The precursor keeps amorphous after being calcined at 600 °C. When calcination temperature exceed 800 °C, significant changes occur and clear peaks appear in the XRD patterns corresponding to crystalline cubic Sc_2O_3 phase (JCPDS43-1028). The result is in agreement with the DTA/TG and FTIR analysis. With the increase of calcination temperature, the peaks become higher and sharper, implying grain growth of the Yb:Sc_2O_3 powders.

Fig. 4 shows the SEM images of the powders obtained by calcining the precursor at different temperatures for 4 h. This is a small crystallites formation and growth process.

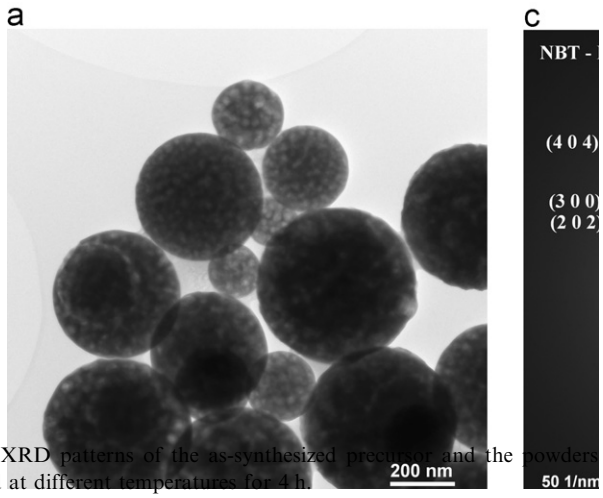

Fig. 3. XRD patterns of the as-synthesized precursor and the powders calcined at different temperatures for 4 h.

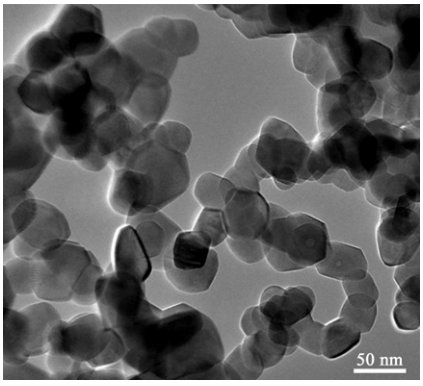

Fig. 5. TEM image of the Yb:Sc_2O_3 powders calcined at 1100 °C for 4 h.

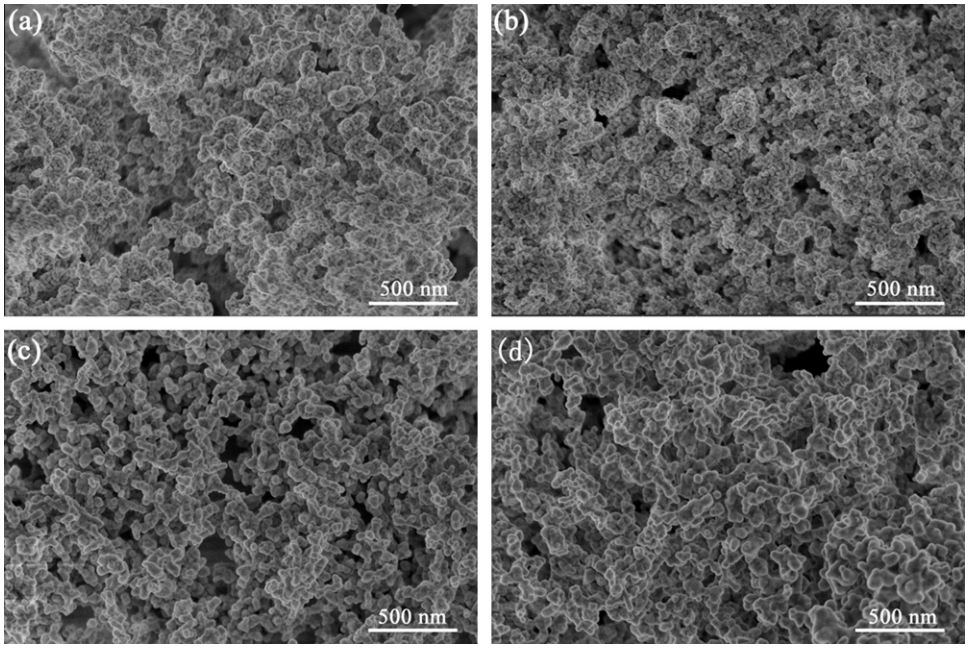

Fig. 4. SEM images of the Yb:Sc_2O_3 powders calcined at (a) 800 °C, (b) 900 °C, (c) 1000 °C and (d) 1100 °C for 4 h.

The mean grain size of the powders calcined at 800 °C is ~20 nm (as shown in Fig. 4a) and increases a little at 900 °C. When the temperature increases further, a significant grain growth is found, as shown in (c and d). Fig. 5 exhibits a TEM image of the powder calcined at 1100 °C for 4 h. The Yb:Sc_2O_3 nanopowders are loosely agglomerated and fairly uniform, with an average particle size of ~35 nm, which accords well with the calculated crystal size of result (~33 nm) from the D_{XRD} result in Fig. 6.

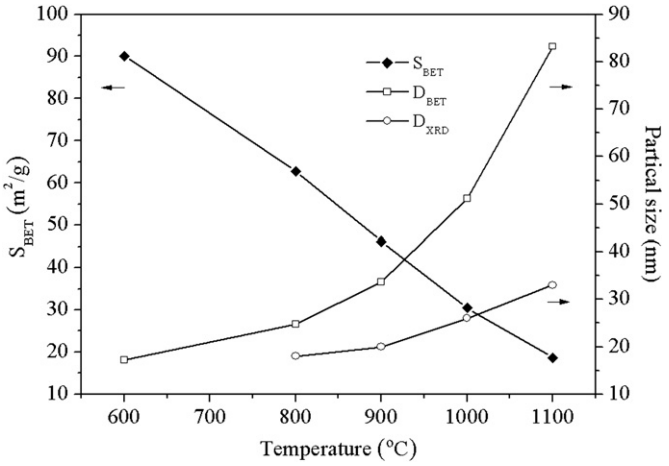

Fig. 6. Dependence of specific surface area and grain size of the Yb:Sc_2O_3 powders on the effect of calcination temperature.

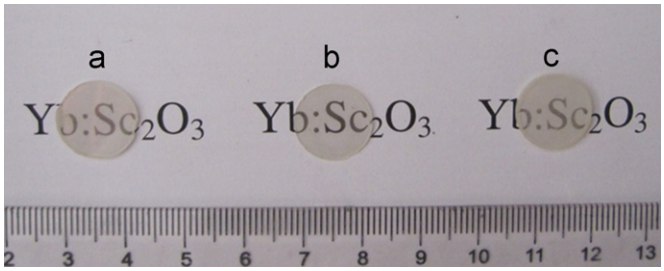

Fig. 7. Photograph of the mirror-polished 5 at% Yb:Sc_2O_3 transparent ceramics (1.0 mm in thickness) fabricated at different temperatures.

Fig. 6 shows the change of the specific surface area (S_{BET}), the corresponding particle size D_{BET} and the crystallite size (D_{XRD}) calculated using Scherrer equation with the calcination temperature. Crystallite size of the Yb:Sc_2O_3 powders is calculated by the X-ray line broadening technique performed on the (2 2 2) diffraction of the Yb:Sc_2O_3 lattice from the Scherrer equation:

$$D_{XRD} = \frac{0.89\lambda}{\beta\cos\theta} \quad (1)$$

where λ is the wavelength of Cu K_α radiation (λ=0.15406 nm) and β is the full-width at half-maximum (FWHM) of a diffraction peak at a Bragg angle θ. The particle size D_{BET} is calculated from the following formula:

$$D_{BET} = \frac{6}{\rho S_{BET}} \quad (2)$$

where ρ (3.68 g/cm^3) is the theoretical density of Yb:Sc_2O_3.

When the calcination temperature increases from 600 to 1100 °C, specific area of Yb:Sc_2O_3 powders reveals a sharp decrease from 90 to 19 m^2/g, corresponding to the increase of the D_{BET} from 17 to 83 nm. The particle size obtained from specific area is about 2.5 times larger than that from XRD method, indicating the existence of considerable agglomeration among primary particles, which can be

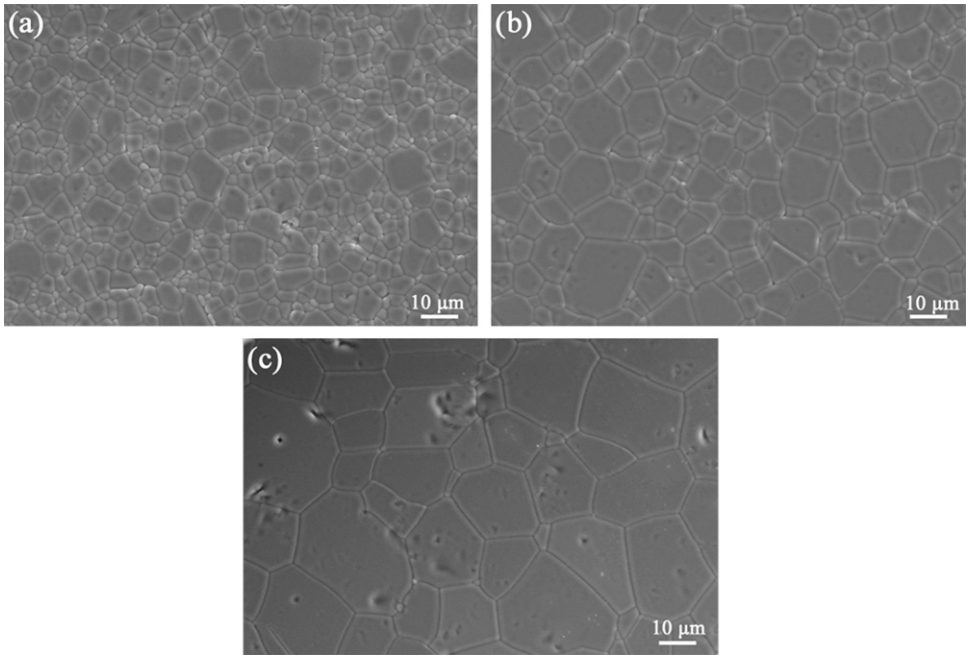

Fig. 8. SEM micrographs of the thermal etched surfaces of the Yb:Sc_2O_3 ceramics fabricated at (a) 1670 °C, (b) 1700 °C, (c) 1730 °C for 20 h under vacuum.

verified by the "necks" between particles shown in the TEM photograph (Fig. 5).

At lower calcination temperature, the powders cannot crystallize completely while higher calcination temperature will cause severely hard agglomeration and decrease the sinterability [17]. In summary, the powders calcined at about 1100 °C for 4 h are highly crystalline, well dispersed, which are suitable for preparation of transparent ceramics with high optical quality.

Fig. 7 shows the photograph of the mirror-polished samples (1 mm in thickness) sintered at 1670, 1700 and 1730 °C for 20 h under $\sim 5 \times 10^{-3}$ Pa vacuum. The result shows that the sintering temperature has a significant effect on the optical qualities of Yb:Sc_2O_3 ceramics. The sample sintered at 1700 °C (Fig. 7b) exhibits the best transparency, whereas the samples sintered at 1670 °C (Fig. 7a) and 1730 °C (c) have somewhat "cloudy" in the center.

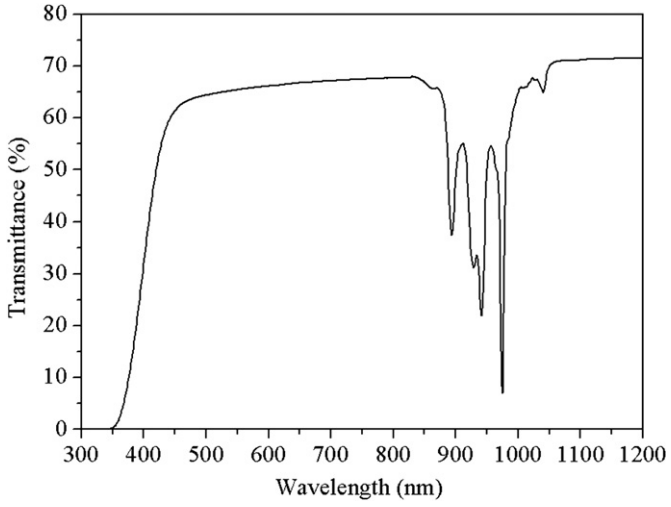

Fig. 9. Optical transmission spectrum of the 5 at% Yb:Sc_2O_3 transparent ceramic (1.0 mm in thickness) fabricated at 1700 °C for 20 h.

Fig. 8 shows SEM micrographs of the thermal etched surfaces of the 5 at% Yb:Sc_2O_3 transparent ceramics. The grain size grows quickly with the increase of sintering temperature. For the sample sintered at 1670 °C, quite a few pores can be seen at the grain boundaries and the average grain size is about 5 μm. The residual pores are gradually removed with the increase of sintering temperature. A dense and almost pore-free microstructure is observed at 1700 °C. The average grain size reaches about 10 μm. Obvious grain growth and inner-grain pore capture happen when the sintering temperature is 1730 °C. The residual pores at the grain boundaries and at the inner grains decrease the optical property of the samples fabricated at 1670 °C (Fig. 7a) and 1730 °C (c).

Fig. 9 shows the transmission spectrum of the 5 at% Yb:Sc_2O_3 transparent ceramic fabricated at 1700 °C for 20 h in the wavelength region of 200–1200 nm. The in-line transmittance of the 5 at% Yb:Sc_2O_3 transparent ceramic (1.0 mm in thickness) increases with the increase of the wavelength and reaches the maximum 71.6% at the wavelength of 1200 nm. The highest transmittance of Sc_2O_3 single crystal is about 79% [8], so it reaches $\sim$90.6% of the theoretical value of Sc_2O_3 single crystals.

Fig. 10 shows the absorption spectrum of the as-fabricated 5 at% Yb:Sc_2O_3 ceramic and the fluorescence spectrum of the sample pumped at the 896 nm wavelength. As shown in Fig. 10a, there are four broad absorption bands around 893, 929, 941, and 974 nm, corresponding to $^2F_{7/2} \rightarrow {}^2F_{5/2}$ transitions. The broad absorption spectrum feature of the Yb:Sc_2O_3 ceramic makes it suitable to be pumped by an LD with no need for accurate temperature control. It can be seen from Fig. 10b that three emission peaks corresponding to $^2F_{5/2} \rightarrow {}^2F_{7/2}$ transitions center at

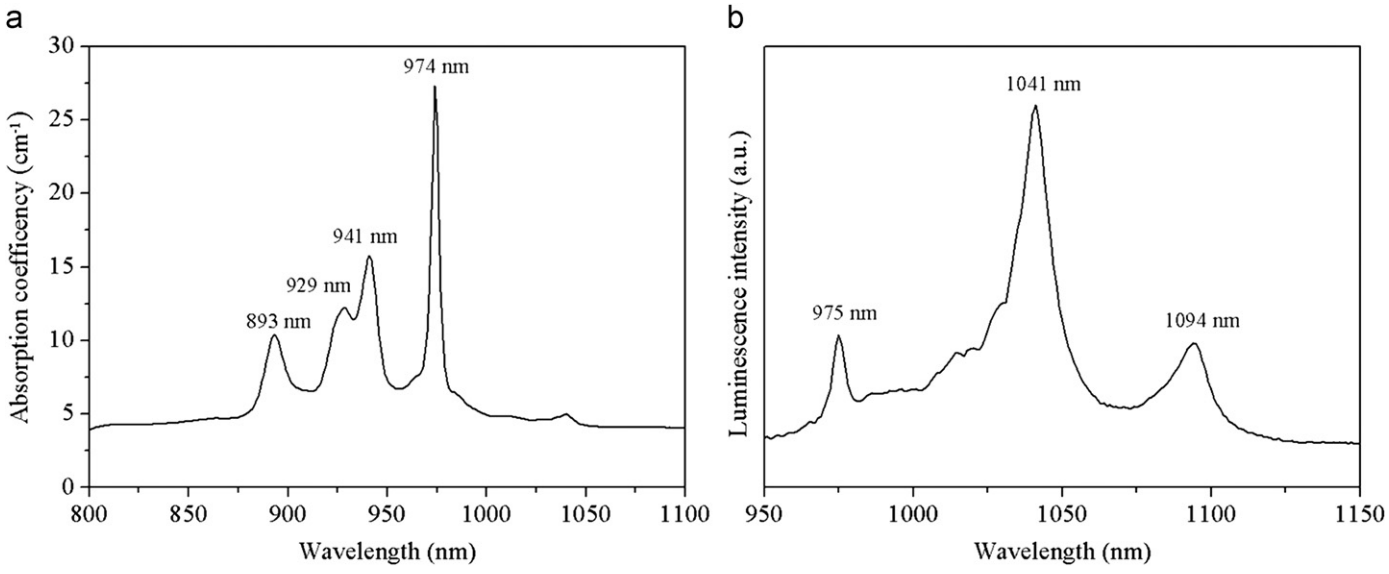

Fig. 10. (a) Room temperature absorption spectrum of the 5 at% Yb:Sc_2O_3 ceramic; (b) fluorescence spectrum of the specimen pumped by the 896 nm LD.

975, 1041 and 1094 nm, respectively. The spectral widths (FWHM, full-width at half-maximum) of Yb:Sc_2O_3 ceramics at 975, 1041 and 1094 nm are about 4.45, 14.69 and 15.47 nm, respectively. The broad emission bands are especially useful in mode-locked laser for ultra-short pulse generation [18].

4. Conclusions

Highly pure, well dispersed and spherical 5 at% Yb:Sc_2O_3 nanopowders with uniform particle size of about 35 nm were synthesized by a novel co-precipitation method, using a mixed solution of $NH_4OH + NH_4HCO_3$ (molar ratio = 3:1) as the precipitant and $(NH_4)_2SO_4$ as the dispersant. Utilizing the synthesized Yb:Sc_2O_3 nanopowders with high sinterability as starting material, high optical quality Yb:Sc_2O_3 transparent ceramics with average grain size of about 10 μm were fabricated by vacuum sintering at 1700 °C for 20 h. The in-line transmittance of the sample with the thickness of 1.0 mm reached 71.6% at the wavelength of 1200 nm, which was 90.6% of the theoretical value of the corresponding single crystal. The spectroscopic results show that Yb:Sc_2O_3 transparent ceramic is a very promising material for high-power short-pulse laser.

Acknowledgements

The work was supported by the Key Program of Shanghai Association of Science and Technology (Grant No. 10JC1416000, 11JC1412400) and the Project for Young Scientists Fund of National Natural Science Foundation of China (Grant No. 51102257, 51002172).

References

[1] M. Tokurakawa, A. Shirakawa, K. Ueda, H. Yagi, T. Yanagitani, A.A. Kaminskii, Diode-pumped sub-100 fs Kerr-lens mode-locked Yb^{3+}:Sc_2O_3 ceramic laser, Optics Letters 32 (2007) 3382–3384.

[2] K. Takaichi, H. Yagi, J. Lu, J.-F. Bisson, A. Shirakawa, K.-i. Ueda, T. Yanagitani, A.A. Kaminskii, Highly efficient continuous-wave operation at 1030 and 1075 nm wavelengths of LD-pumped Yb^{3+}:Y_2O_3 ceramic lasers, Applied Physics Letters 84 (2004) 317–319.

[3] N.L. Wang, X.Y. Zhang, Z.H. Bai, Q.S. Liu, L.P. Lu, X.Y. Mi, H.Y. Sun, X.C. Wang, Carbonate-precipitation synthesis of Yb^{3+}:Y_2O_3 nanopowders and its characteristics, Powder Technology 203 (2010) 458–461.

[4] P. Klopp, V. Petrov, U. Griebner, K. Petermann, V. Peters, G. Erbert, Highly efficient mode-locked Yb:Sc_2O_3 laser, Optics Letters 29 (2004) 391–393.

[5] V. Lupei, A. Lupei, A. Ikesue, Transparent Nd and (Nd, Yb)-doped Sc_2O_3 ceramics as potential new laser materials, Applied Physics Letters 86 (2005) 111118.

[6] J.G. Li, T. Ikegami, T. Mori, Fabrication of transparent Sc_2O_3 ceramics with powders thermally pyrolyzed from sulfate, Journal of Materials Research 18 (2003) 1816–1822.

[7] D. Grosso, P.A. Sermon, Scandium oxide nanoparticles produced from sol–gel chemistry, Journal of Materials Chemistry 10 (2000) 359–363.

[8] J.G. Li, T. Ikegami, T. Mori, Fabrication of transparent, sintered Sc_2O_3 ceramics, Journal of the American Ceramic Society 88 (2005) 817–821.

[9] J.G. Li, T. Ikegami, T. Mori, Y. Yajima, Wet-chemical routes leading to scandia nanopowders, Journal of the American Ceramic Society 86 (2003) 1493–1499.

[10] Z. Xiu, J.G. Li, X.D. Li, D. Huo, X.D. Sun, T. Ikegami, T. Ishigaki, Nanocrystalline scandia powders via oxalate precipitation: the effects of solvent and solution pH, Journal of the American Ceramic Society 91 (2008) 603–606.

[11] Y. Wang, B. Lu, X. Sun, T. Sun, H. Xu, Synthesis of nanocrystalline Sc_2O_3 powder and fabrication of transparent Sc_2O_3 ceramics, Advances in Applied ceramic 110 (2011) 95–98.

[12] J.G. Li, T. Ikegami, T. Mori, Y. Yajima, Monodispersed Sc_2O_3 precursor particles via homogeneous precipitation: synthesis, thermal decomposition, and the effects of supporting anions on powder properties, Journal of Materials Research 18 (2003) 1149–1156.

[13] M. Galceran, M.C. Pujol, J.J. Carvajal, X. Mateos, C. Zaldo, M. Aguiló, F. Díaz, Structural characterization and ytterbium spectroscopy in Sc_2O_3 nanocrystals, Journal of Luminescence 130 (2010) 1437–1443.

[14] Q.W. Chen, Y. Shi, L.Q. An, S.W. Wang, J.Y. Chen, J.L. Shi, A novel co-precipitation synthesis of a new phosphor Lu_2O_3:Eu^3, Journal of the European Ceramic Society 27 (2007) 191–197.

[15] K. Serivalsatit, B. Kokuoz, B. Yazgan-Kokuoz, M. Kennedy, J. Ballato, Synthesis, processing, and properties of submicrometer-grained highly transparent yttria ceramics, Journal of the American Ceramic Society 93 (2010) 1320–1325.

[16] D. Grosso, P.A. Sermon, Scandium oxide nanoparticles produced from sol–gel chemistry, Journal of Materials Chemistry 10 (2000) 359–363.

[17] J. Li, F. Chen, W.B. Liu, W.X. Zhang, L. Wang, X.W. Ba, Y.J. Zhu, Y.B. Pan, J.K. Guo, Co-precipitation synthesis route to yttrium aluminum garnet (YAG) transparent ceramics, Journal of the European Ceramic Society 32 (2012) 2971–2979.

[18] D.W. Luo, J. Zhang, C.W. Xu, X.P. Qin, D.Y. Tang, J. Ma, Fabrication and laser properties of transparent Yb:YAG ceramics, Optical Materials 34 (2012) 936–939.